

# Chameleon Gravity, Electrostatics, and Kinematics in the Outer Galaxy

R. Pourhasan<sup>(a)\*</sup>, N. Afshordi<sup>(b,a)†</sup>, R. B. Mann<sup>(a,b)‡</sup> and A. C. Davis<sup>(c)§</sup>

<sup>(a)</sup> *Department of Physics & Astronomy,*

*University of Waterloo, Waterloo, Ontario N2L 3G1, Canada*

<sup>(b)</sup> *Perimeter Institute for Theoretical Physics,*

*31 Caroline St. N., Waterloo, ON, N2L 2Y5, Canada*

<sup>(c)</sup> *Department of Applied Mathematics and Theoretical Physics,*

*Center for Mathematical Sciences, Cambridge CB3 0WA, United Kingdom*

Light scalar fields are expected to arise in theories of high energy physics (such as string theory), and find phenomenological motivations in dark energy, dark matter, or neutrino physics. However, the coupling of light scalar fields to ordinary (or dark) matter is strongly constrained from laboratory, solar system, and astrophysical tests of fifth force. One way to evade these constraints in dense environments is through the chameleon mechanism, where the field’s mass steeply increases with ambient density. Consequently, the chameleonic force is only sourced by a thin shell near the surface of dense objects, which significantly reduces its magnitude.

In this paper, we argue that thin-shell conditions are equivalent to “conducting” boundary conditions in electrostatics. As an application, we use the analogue of the method of images to calculate the back-reaction (or self-force) of an object around a spherical gravitational source. Using this method, we can explicitly compute the violation of equivalence principle in the outskirts of galactic haloes (assuming an NFW dark matter profile): Intermediate mass satellites can be slower than their larger/smaller counterparts by as much as 10% close to a thin shell.

---

\* email address: r2pourha@uwaterloo.ca

† email address: nafshordi@perimeterinstitute.ca

‡ email address: rbmann@sciborg.uwaterloo.ca

§ email address: A.C.Davis@damtp.cam.ac.uk

## I. INTRODUCTION

Cosmological observations indicate that the universe is accelerating today with about 75 percent of the energy density in dark energy<sup>1,2</sup>. If the dark energy is a scalar field then its mass needs to be very light indeed, but its couplings to ordinary matter must be suppressed to avoid fifth force constraints. Indeed fifth force experiments such as the Cassini satellite experiment put stringent bounds on the gravitational coupling of nearly massless scalar fields<sup>3-6</sup>. The chameleon scenario posits that a scalar field with gravitational strength couplings to matter could generate the present day acceleration, but evade fifth force constraints<sup>7</sup>. The properties of the scalar field depend on the ambient density. In particular its mass is density dependent. Cosmologically the chameleon mass can be of order the Hubble constant, allowing the field to be rolling on cosmological time-scales<sup>8</sup>. However, in the solar system the chameleon can be sufficiently massive so that it evades fifth force constraints. Indeed, chameleon theories have a non-trivial way of evading empirical gravitational constraints via the existence of a thin-shell mechanism. For sufficiently large objects the chameleonic force is almost entirely due to a thin-shell of matter just below the surface of the object, with the matter in the core of the object giving a negligible contribution to the force. Although the original papers assumed the coupling to matter was of gravitational strength, it was later realized that, due to non-linear effects, the coupling could be much larger whilst still preserving the properties of the chameleon mechanism<sup>9</sup>.

The chameleon mechanism has been tested in many different situations and constraints placed on the parameters of the theory<sup>10,11</sup>. Gravitational tests in the solar system<sup>7</sup> and the full cosmological evolution have been studied<sup>8</sup>. The effect it has on structure formation on sub-galactic scales<sup>13</sup> and on large scale structure formation have also been investigated<sup>14</sup>. More recently the chameleon coupling to photon fields has been investigated and constraints have been placed on the mechanism from laboratory experiments<sup>12</sup> and astrophysical measurements<sup>15</sup>. Laboratory experiments have been designed to look for the chameleonic force between objects<sup>16</sup>. These experiments are similar, though distinct, to Casimir force experiments and should either detect the chameleonic force or severely constrain it in the near future.

On cosmological scales, the introduction of a chameleonic force can lead to violations of the equivalence principle, as objects with shallow potential wells (or small velocity dis-

persions) fall at a higher acceleration than the larger object that have a thin shell<sup>17</sup>. The chameleon effect on CDM large scale structure can now be explicitly seen in numerical simulations of  $f(R)$  gravity models<sup>18–20</sup>

One effect that has not been studied is the chameleonic back-reaction on galactic scale objects. In chameleon theories large galactic haloes should have a thin shell. In particular, the Navarro-Frenk-White (or NFW) profile models the dark matter distribution in galactic haloes<sup>21</sup>. In this paper, we investigate the back-reaction (or self-force) of satellites moving in the halo outskirts of an NFW profile, which can lead to observable violations of the equivalence principle. To do this, we use an analogy between chameleon thin-shell conditions and electrostatics, which enables an application of the method of images to fifth-force calculations (This analogy was also recently noticed in<sup>22</sup>, and used to argue the presence of ‘lightning rod’ effects close to non-spherical thin shells).

The plan of this paper is as follows: In the next section, we review the chameleon mechanism, explain how its field depends on the ambient density, and how the thin shell mechanism works in this context. We then compare the thin shell mechanism with electrostatics in Sec. III, showing that there is an analogy. This analogy enables us to use the method of images to compute the chameleonic back-reaction (or self-force). We compute the self-force corrections to the fifth force between a test object and a body with a thin shell before going on to consider the NFW profile and the chameleon force in Sec. IV. In Sec. V, we show that the circular velocity of intermediate mass satellites in the outer halo can be reduced significantly if the back-reaction is taken into account. Finally, Sec. VI contains a discussion of our results and concludes the paper.

## II. THE CHAMELEON MECHANISM

Chameleon fields appear in scalar-tensor theories of gravity. The action of the chameleon field in the Einstein frame is

$$S = \int d^4x \sqrt{-g} \left[ \frac{M_p^2}{2} R - \frac{1}{2} (\partial\phi)^2 - V(\phi) \right] \quad (1)$$

where  $M_p = (8\pi G)^{-1/2}$  is the reduced Planck mass. Matter couples to both gravity and the scalar field according to

$$S_m(\psi, A^2(\phi)g_{\mu\nu}), \quad (2)$$

where  $\psi$  is a matter field and  $A$  the conformal factor relating the Jordon and Einstein frame metrics. Notice that the scalar field couples to all matter species, including baryons. This conformal coupling gives an extra contribution to the Klein-Gordon equation.

$$\nabla^2\phi = V_{,\phi} - \alpha_\phi T^\mu{}_\mu, \quad (3)$$

where  $\alpha_\phi \equiv \frac{\partial \ln A}{\partial \phi}$ . In the approximation that matter is well described by a pressureless, perfect fluid this becomes

$$\nabla^2\phi = V_{,\phi} + \alpha_\phi \rho_m A(\phi) \quad (4)$$

where  $\rho_m$  is the matter density.

An immediate consequence is that the dynamics of  $\phi$  is governed by the effective potential, which depends explicitly on the density,

$$V_{eff} = V(\phi) + \rho_m A(\phi). \quad (5)$$

If the bare potential is of a runaway form,

$$V(\phi) = \frac{\Lambda^{4+n}}{\phi^n}, \quad (6)$$

where  $\Lambda$  is a parameter with dimensions of mass and the conformal factor increases with  $\phi$ , for example as

$$A(\phi) = \exp(\beta\phi/M_p), \quad (7)$$

then the effective potential has a minimum that depends on the density. Thus the physical properties of the field depend on the ambient density.

From the above we can see that the mass of the chameleon is an increasing function of the density such that it can be massive in dense environments, but nearly massless cosmologically. Also, the non-linearity in the chameleon equation of motion gives rise to the thin-shell mechanism, which is discussed in the next section. The net effect of these properties is that chameleon fields evade detection via gravitational tests for fifth forces, but can play the role of dark energy.

### III. THIN-SHELLS, ELECTROSTATIC CONDUCTORS, AND THE CHAMELEON FIFTH FORCE

It is well-known from electrostatics that to find the backreaction of a charge on electric potential close to a conducting sphere one may use the method of images. Here we consider

the analogous problem for the chameleon mechanism, in that we consider the backreaction of a test body close to a thin-shell body that is a ‘‘chameleon conductor’’ . The method of images will be effective insofar as the conductor approximation is valid, which in turn (as we argue) implies that the shell is sufficiently thin.

Let us first summarize the chameleon properties close to a compact, spherical body with a thin shell. The chameleon field inside a body of radius  $R_c$  with a thin shell is<sup>7</sup>

$$0 < r < R_{\text{roll}} : \quad \phi \approx \phi_c, \quad (8)$$

$$R_{\text{roll}} < r < R_c : \quad \phi_{\text{int}} = \frac{\beta\rho_c}{3M_p} \left( \frac{r^2}{2} + \frac{R_{\text{roll}}^3}{r} \right) - \frac{\beta\rho_c R_{\text{roll}}^2}{2M_p} + \phi_c, \quad (9)$$

where  $M_p = (8\pi G)^{-1/2}$ ,  $\phi_c$  is the value of the field inside the compact body of density  $\rho_c$  and radius  $R_c$ , while  $R_{\text{roll}}$  is the radius where the field starts to move from its value inside the compact body. To make the above two approximations have assumed:

$$M_p |V_{,\phi}| \ll \beta\rho_c e^{\beta\phi/M_p} \longrightarrow V_{,\phi} \text{ is negligible}, \quad (10)$$

$$\beta\phi/M_p \ll 1 \longrightarrow e^{\beta\phi/M_p} \approx 1. \quad (11)$$

We can write the field at the surface of the body, i.e.  $r = R_c$ , as

$$\phi_s \equiv \phi(R_c) = \frac{\beta\rho_c}{3M_p} \left( \frac{R_c^2}{2} + \frac{R_{\text{roll}}^3}{R_c} \right) - \frac{\beta\rho_c R_{\text{roll}}^2}{2M_p} + \phi_c. \quad (12)$$

If we are in the thin-shell regime, then

$$\frac{\Delta R_c}{R_c} \approx \frac{R_c - R_{\text{roll}}}{R_c} \ll 1 \quad (13)$$

and using a Taylor expansion, eq. (12) reduces to

$$\phi_s - \phi_c = \frac{\beta\rho_c}{2M_p} (\Delta R_c)^2. \quad (14)$$

Inserting the Newtonian potential

$$\Phi_N = \frac{1}{8\pi M_p^2} \frac{M_c}{R_c} = \frac{\rho_c R_c^2}{6M_p^2} \quad (15)$$

into eq. (14) we obtain

$$\frac{\phi_s - \phi_c}{3\beta M_p \Phi_N} = \left( \frac{\Delta R_c}{R_c} \right)^2, \quad (16)$$

which provides a criterion for comparing the value of the field at the surface relative to its interior in terms of the thickness of the shell. Whilst the above has been derived using

approximations, it has been checked analytically and numerically in the original papers, both for  $\beta = O(1)^7$  and in the strong coupling regime<sup>9</sup>. Using (13), we see that the field values are nearly the same, i.e. the field is continuous across the thin shell. Therefore, ignoring the outside chameleon mass, the problem becomes analogous to that of a conductor held at fixed potential in electrostatics, where  $\phi$  takes a fixed value inside,  $\phi_c$ , while satisfying the Laplace equation outside the object. As a result, the back-reaction problem can be treated analogously to that of a conducting sphere in electrostatics.

In obtaining the total force between a spherical body with a thin-shell and a test object without a thin-shell, we have three types of forces to consider.

- The net gravitational force from a density distribution  $\rho(r)$  of the thin-shell body acting on a test object of mass  $m$ . This is given by

$$\vec{F}_G = -\frac{m}{M_p} \vec{\nabla} \phi_G(r), \quad (17)$$

where  $\phi_G$  is the gravitational potential satisfying:

$$\nabla^2 \phi_G = \frac{\rho(r)}{2M_p}. \quad (18)$$

- The chameleonic force acting on a test object of mass  $m$  coupled with strength  $\beta$  to a chameleon field  $\phi(r)$  of a body with a thin-shell of mass  $M$ . Here the relevant force is<sup>7</sup>

$$\vec{F}_\phi = -\frac{\beta}{M_p} m \vec{\nabla} \phi(r). \quad (19)$$

Inserting the external solution for a thin-shell rigid body of radius  $R_c$

$$\phi_{ext}(r) = -\frac{\beta}{4\pi M_p} \frac{\widetilde{M} e^{-m_\infty r}}{r} + \phi_\infty, \quad r > R_c \quad (20)$$

and ignoring the exponential factor (since  $m_\infty R_c \ll 1$ ) the chameleon force (or fifth force) can be written as

$$\vec{F}_\phi = -\alpha \frac{m \widetilde{M}}{r^2} \hat{r} \quad (21)$$

where  $\alpha = \beta^2/4\pi M_p^2$  and  $r$  is the distance between the centers of the bodies. We have introduced  $\widetilde{M}$  as the reduced mass of the thin-shell body with radius  $R_c$  and mass  $M$

$$\widetilde{M} = \frac{3\Delta R_c}{R_c} M, \quad (22)$$

where

$$\frac{\Delta R_c}{R_c} = \frac{\phi_\infty - \phi_c}{6\beta M_p \Phi_N}, \quad (23)$$

where  $\Phi_N = M_c/8\pi M_p^2 R_c$  is the Newtonian potential,  $\phi_\infty$  minimizes the effective potential outside the thin-shell body and  $\phi_c$  minimizes the effective potential inside the thin-shell body which can be obtained as:

$$\phi_\infty = \left( \frac{\Lambda^5 M_p}{\beta \rho_\infty} \right)^{1/2}, \quad \phi_i = \left( \frac{\Lambda^5 M_p}{\beta \rho_c} \right)^{1/2}, \quad (24)$$

where we have used (6) with  $n = 1$  in the above and the density far away from the body with the thin-shell is  $\rho_\infty$ , whilst the density inside the body is  $\rho_c$ .

- The back reaction force between the thin-shell body and test object. As noted above, this can be obtained using method of images, yielding

$$\delta \vec{F} = -\frac{1}{8\pi M_p^2} \frac{mm'}{(r-r')^2} \hat{r}, \quad (25)$$

where  $m'$  is the image mass of the test body located at  $r'$  inside the thin-shell body of radius  $R_c$ :

$$m' = -\frac{mR_c}{r}, \quad r' = \frac{R_c^2}{r}. \quad (26)$$

Note that we have neglected the chameleon mass exterior to the thin-shell body, since this mass depends on the density of the environment and the density outside the body is assumed to be small (this will change in the next section, where we assume a diffuse NFW profile). Accordingly, the total force acting on the test body  $m$  from the thin-shell body  $M$ , including both the fifth force and back reaction, is

$$\vec{F}_T = \vec{F}_G + \vec{F}_\phi + \delta \vec{F}. \quad (27)$$

To summarize, the test object responds to not only the fifth force from the thin shell, but also to its own image reflected from the thin shell. While the primary fifth force is attractive, the back-reaction (or self-force) is repulsive, as the image has the opposite charge (i.e. negative mass). Moreover, the self-force will become comparable to the primary force as test object approaches the thin shell.

#### IV. NFW PROFILE AND CHAMELEON FORCE

In this section we will obtain the chameleon force for a dark matter halo (similar to that of the Milky Way galaxy) acting on a test body by considering the NFW profile for the halo density<sup>21</sup>, which is of the form

$$\rho(r) = \frac{\rho_s}{\frac{r}{r_s}(1 + \frac{r}{r_s})^2} \quad (28)$$

where  $r_s = 10 \text{ kpc} = 1.57 \times 10^{27} \text{ eV}^{-1}$ . The quantity  $\rho_s$  is given by

$$\int_0^{300 \text{ kpc}} 4\pi r^2 \rho(r) dr = 200 \bar{\rho}_c \left[ \frac{4\pi}{3} (300 \text{ kpc})^3 \right] \quad (29)$$

where  $\bar{\rho}_c = 3H_0^2 M_p^2$  is the critical density of the universe. Using the present Hubble constant  $H_0 \simeq 71 \text{ km/s/Mpc} = 1.5 \times 10^{-33} \text{ eV}$  and the reduced Planck mass  $M_p = (8\pi G)^{-1/2} = 2.43 \times 10^{27} \text{ eV}$  we obtain

$$\rho_s = 3.0 \times 10^{-5} \text{ eV}^4.$$

We also consider the potential as in Eq. (6).

Next we divide the space into two distinct regions.

**I)** The interior region. Here the following constraint

$$\frac{M_p \nabla^2 \phi}{\beta \rho(r)} \ll 1 \quad (30)$$

is satisfied, and so the chameleon equation becomes

$$\nabla^2 \phi = V_{,\phi} + \frac{\beta \rho(r)}{M_p} e^{\beta \phi / M_p}. \quad (31)$$

Neglecting  $\nabla^2 \phi$  and solving

$$\frac{\beta \rho(r)}{M_p} + V_{,\phi} = 0 \quad (32)$$

where the exponential coefficient has been ignored since we have assumed  $\beta \phi / M_p \ll 1$ , we find

$$\phi_{int}(x) \approx \phi_s [x(1+x)^2]^{1/(n+1)}, \quad x_{0<} < x < x_{0>} \quad (33)$$

for the solution to eq. (32). For convenience we have defined the dimensionless variable  $x = r/r_s$  and

$$\phi_s = \left( \frac{n \Lambda^{n+4} M_p}{\beta \rho_s} \right)^{1/(n+1)}. \quad (34)$$



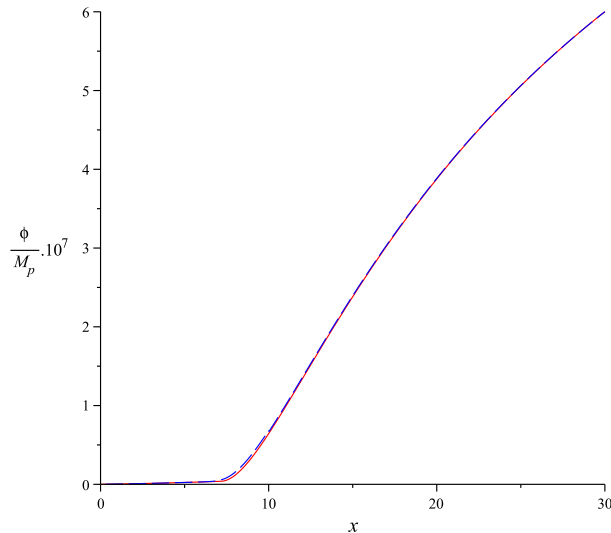


FIG. 1: Chameleon field  $\phi$  versus distance  $x = r/r_s$ , where the red solid line shows the analytic solution and the blue dashed one depicts the numeric solution.

The quantities  $x_{0<}$  and  $x_{0>}$  respectively denote the lower and upper values of  $x$  that beyond which the constraint (30) is no longer valid. We can find these values by setting  $\frac{M_p \nabla^2 \phi}{\beta \rho} = 0.01$ , and then solving numerically for the two real roots  $x_{0<}$  and  $x_{0>}$ .

**II)** The exterior region. Here we impose the condition

$$V_{,\phi} \ll \nabla^2 \phi$$

which we take to be valid for  $x > x_c$ . The exterior solution can therefore be found by neglecting the potential term in the chameleon equation

$$\nabla^2 \phi_{ext}(x) = \frac{\beta r_s^2 \rho(x)}{M_p}, \quad (35)$$

yielding

$$\phi_{ext}(x) \approx -\frac{B \ln(1+x)}{x} - \frac{C}{x} + \phi_\infty, \quad x > x_c \quad (36)$$

with

$$B = \frac{\beta \rho_s r_s^2}{M_p}, \quad (37)$$

where  $C$  and  $\phi_\infty$  are integration constants.

The quantity  $\phi_\infty$  can be interpreted as the minimum of chameleon field for  $x \gg x_c$ . However, we need some criterion for determining  $C$  and  $x_c$ . Recalling that at  $x = x_{0>}$

the chameleon field starts to deviate from the interior constraint (30) and that the exterior solution is valid for  $x \geq x_c$ , we find that if we demand

$$\frac{x_c - x_{0>}}{x_c} \ll 1 \quad (38)$$

then to a very good degree of approximation the interior solution is still valid inside the shell  $x_{0>} < x < x_c$ , and the shell can be considered as sufficiently thin. Hence to compute the integration constant  $C$  we match the interior and exterior solutions and their derivatives at  $x = x_c$ , which yields

$$C = -B \ln(1 + x_c) + \phi_\infty x_c - \phi_s [x_c(1 + x_c)^2]^{1/(n+1)} x_c, \quad (39)$$

where  $x_c$  is the smaller real root of the following equation

$$[x_c(1 + x_c)^2]^{1/(n+1)} = \frac{(n+1)}{\phi_s} \frac{(1 + x_c)\phi_\infty - B}{(n+4)x_c + n + 2} \quad (40)$$

which can be solved numerically for given parameters  $n$ ,  $\beta$ ,  $\Lambda$  and  $\phi_\infty$ .

For simplicity we henceforth set  $n = 1$  and take  $\beta$  of order unity. Whilst we could work with different parameters and in the strong coupling regime, we would not expect our results to change qualitatively, as long as the thin-shell conditions are satisfied. Then the only parameters left to be determined are  $\phi_\infty$  and  $\Lambda$ . We determine these via two basic considerations. First, the thin-shell conditions (30) and (38) must be satisfied, where the former yields an upper bound for  $\Lambda$  of the order of 10 eV. Second, since the size of the halo is approximately 300 kpc then the values for  $\phi_\infty$  and  $\Lambda$  must imply that the smaller real root of eq. (40) be in a range between  $0 < R_c < 300$  kpc, where  $R_c = (10 \text{ kpc})x_c$ . Numerically we find that the second consideration along with the upper bound on  $\Lambda$  imply the upper bound for  $\phi_\infty$  is of the order of  $10^{-5}M_p$ . Hence we choose  $\phi_\infty = 1.5 \times 10^{-6}M_p$  and  $\Lambda = 4.66$  eV, which satisfies all considerations simultaneously, yielding  $x_c = 7.183^{27}$ .

We now proceed to solve the whole chameleon equation numerically, using the information from our semi-analytic investigation thus far. Specifically, setting  $n = 1$ ,  $\beta = 1$  and  $\Lambda = 4.66$  eV yields

$$\frac{1}{x^2} \frac{d}{dx} \left( x^2 \frac{d\tilde{\phi}(x)}{dx} \right) = \frac{\beta \rho_s r_s^2}{M_p^2 x (1+x)^2} e^{\beta \tilde{\phi}(x)} - \frac{n \Lambda^{n+4} r_s^2}{M_p^{n+2} \tilde{\phi}(x)^{n+1}} \quad (41)$$

while we have re-scaled  $\phi/M_p \rightarrow \tilde{\phi}$ . We present our numerical and semi-analytical solutions in fig. (1).

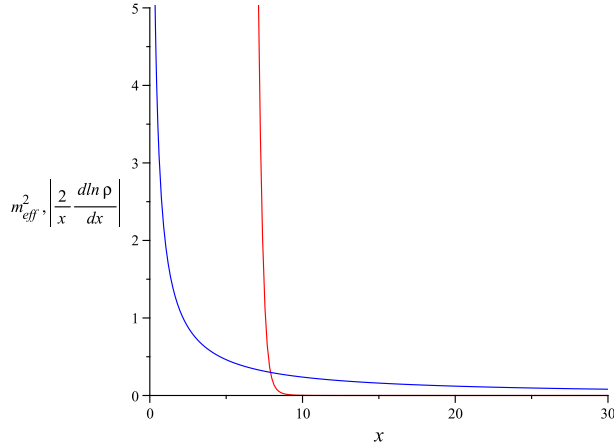


FIG. 2: The effective mass of the chameleon field (red) and  $|\frac{2}{x} \frac{d \ln \rho}{dx}|$  (blue) versus distant  $x = r/r_s$ . It is clear that for the internal region  $x < x_c = 7.183$  we have  $m_{eff}^2 \gg |\frac{2}{x} \frac{d \ln \rho}{dx}|$ .

It is evident that the numerical and semi-analytic solutions match with high accuracy, confirming the approximations we made for this choice of parameters. For example, one approximation neglected the mass of the chameleon field in the external region. Fig. (2) shows the effective mass of the chameleon, i.e.  $m_{eff}^2 = d^2 V_{eff}(\phi)/d\phi^2$ , versus distant  $x$ . Here we see that the chameleon mass almost vanishes for  $x > x_c$ , and that  $m_{eff}^2 \gg |\frac{2}{x} \frac{d \ln \rho}{dx}|$  for the interior region. The latter inequality is an equivalent expression for the interior constraint (30): taking the derivative with respect to  $r$  from Eq. (32) gives  $m_{eff}^2 = -\beta \rho' / \phi' M_p$  where  $\phi$  is the interior solution given by eq. (33).

In the next section, we use our semi-analytic solutions (33) and (36), to obtain physical quantities such as the fifth force, its back-reaction, and their possible observational consequences.

## V. CIRCULAR VELOCITY FROM FIFTH FORCE WITH BACK REACTION

In this section, as an application of the thin-shell framework developed above, we will obtain the circular velocity of orbiting satellite galaxies in the exterior region of the galactic haloes, caused by the gravitational force, the fifth force and the back-reaction. Since by the constraint (38) we demanded the shell of the halo to be thin, we will use the method of images which takes into account the back-reaction effect of the satellites.

Furthermore, for simplicity, we limit ourselves to those satellites in the galaxy that can

reasonably be considered as bodies *without* a thin-shell. For these satellites we have

$$\frac{\phi_{ext}(x) - \phi_c}{6\beta M_p \Phi_N} > 1, \quad (42)$$

where  $\phi_{ext}(x)$  is the external chameleon field (36) calculated at the satellite location. Since the virial velocity of a satellite is  $v_{vir}^2 \propto \Phi_N$ , the condition (42) yields a constraint on the virial velocity

$$v_{vir}^2 < \frac{\phi_{ext}(x)}{6\beta M_p} \quad (43)$$

where we have neglected  $\phi_c$ , which is the minimum of the chameleon field inside the rigid body. For our choice of NFW halo and coupling parameters, this reduces to  $v_{vir} \lesssim 10$ -15 km/s, close to the thin shell, which is a typical velocity dispersion for intermediate mass satellites of Milky Way.

Inserting the NFW profile (28) for the density distribution of the halo in the eq. (17), the net gravitational force (that is finite at the origin) is

$$\vec{F}_G = -\frac{m}{M_p r_s} \left[ -\frac{\tilde{B}}{x(1+x)} + \frac{\tilde{B} \ln(1+x)}{x^2} \right] \hat{r} \quad (44)$$

where  $\tilde{B} = \rho_s r_s^2 / 2M_p$ .

The fifth force acting on a test object of mass  $m$  caused by the thin-shell halo can be obtained from eqs. (19) and (33) for the interior region as

$$\vec{F}_{\phi_{int}} = -\frac{\beta m}{M_p r_s} \left[ \frac{1+3x}{x(1+x)(1+n)} \phi_{int} \right] \hat{r} \quad x < x_c \quad (45)$$

or from (36)

$$\vec{F}_{\phi_{ext}} = -\frac{\beta m}{M_p r_s} \left[ \frac{C}{x^2} - \frac{B}{x(1+x)} + \frac{B \ln(1+x)}{x^2} \right] \hat{r} \quad x > x_c \quad (46)$$

for the exterior region.

The force caused by the back-reaction effect is simply the radial force between the test object  $m$  and its image mass  $m'$ , located at  $r'$  inside the thin-shell halo. This is given by eqs. (25) and (26) as

$$\delta \vec{F} = \left( \frac{m^2}{8\pi M_p^2 r_s^2} \right) \frac{x_c x}{(x^2 - x_c^2)^2} \hat{r} \quad (47)$$

where we have used the dimensionless radial coordinate  $x = r/r_s$  and  $x_c$  is the smaller real root in eq. (40). Finally, the total force is

$$\vec{F}_T = \vec{F}_G + \vec{F}_\phi + \delta \vec{F}, \quad (48)$$

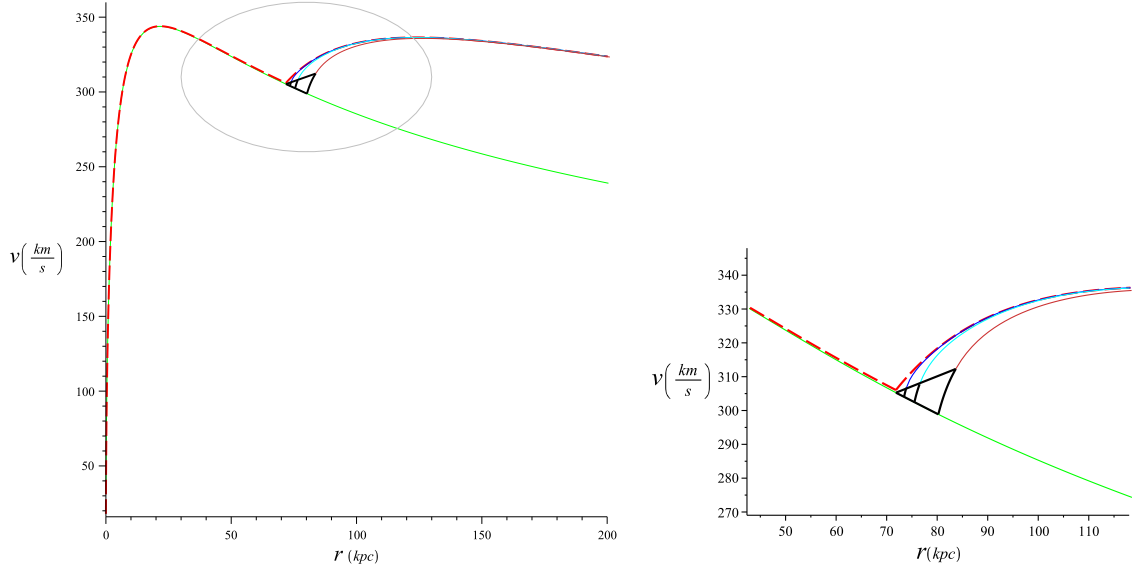


FIG. 3: Circular velocity versus distance from the center of the galactic halo. The green solid line is obtained by considering the net gravitational force while the red dashed one is obtained by considering the correction from including the fifth force. For the rest, the correction due to the back-reaction has been also taken into account. The mass of the test object increases from top to bottom:  $m = 10^8 M_\odot$  (blue),  $m = 10^9 M_\odot$  (cyan),  $m = 10^{10} M_\odot$  (brown).

which is the sum of the net gravitational force (44), the fifth force (45)/(46) and the image force (47).

From the radial force we may obtain the circular velocity  $v(r) = \sqrt{|\vec{F}|r/m}$  as a function of  $r$ , the distance from center of the halo. Including only the fifth force, it is easy to see that the circular velocity is the same for all the objects in the external region of the halo, i.e. it is independent of the mass of the test object. This changes once the back-reaction is taken into account, which is shown in Fig. (3). For example, we see that for an object with mass of the order  $10^{10} M_\odot$ , considering just gravitational force from NFW profile we will obtain the green line for the circular velocity. If we include the fifth force from the chameleon theory for the NFW profile we get the red dashed line, which has a negligible effect in the interior region, but manifestly changes the exterior behaviour. Including next the back-reaction we obtain the brown line, which clearly deviates from the dashed red one for a large satellite mass. For smaller masses the deviation is not as big: in fact, it is clear that the correction from the image force becomes less important as the mass of the satellite decreases. The region enclosed by the black triangle denotes the regime in which the back-reaction becomes

50%–100% of the original fifth-force. Therefore, we cannot trust our approximations (which neglected the effect of satellite on the thin shell); the velocity should lie somewhere inside the triangle, which specifies the range of uncertainty in our prediction. This triangle region grows as the mass of the test body increases, a feature more vivid in the close-up.

An interesting observational window into violations of equivalence principle on Galactic scales was introduced in<sup>23–25</sup>, where it was argued that leading and trailing tidal streams of satellites of Milky Way would be asymmetric, if stars and dark matter (that dominates these galaxies) experienced different gravitational accelerations. Based on the symmetry of the tidal streams of the Sagittarius dwarf galaxy,<sup>23</sup> argue that the difference between these accelerations should be  $< 10\%$ , which implies  $< 5\%$  difference in circular velocities. Given that  $v_{\text{vir}} \sim 15$  km/s, and  $M \sim 10^9 M_{\odot}$  for Sagittarius dwarf<sup>26</sup>, we expect around 3% difference in circular velocities (see Fig. 3), which is just below the observational limit, assuming that Sagittarius orbit is just outside a chameleon thin shell. However, further improvements in these limits, and/or study of other tidal streams in the Milky Way halo could well provide a way to discover this effect in the outer Galaxy.

## VI. CONCLUSIONS

In chameleon theories there is a fifth force, which is suppressed due to the chameleonic effect and the thin shell. In this work, for the first time, we have quantified the proper thin shell conditions in chameleon gravity for the dark matter haloes surrounding galaxies (such as Milky Way), assuming an NFW density profile. As a result we could obtain the chameleon force for such a profile, which adds to the net gravitational force. We showed that this additional fifth force manifestly changes the behaviour of the circular velocity for the test objects in the exterior region of the halo.

Since chameleon gravity is non-linear, the addition of a test object can change the chameleon field, and thus lead to a back-reaction or self-force, an effect that has never been calculated explicitly. In this paper, we have calculated this back-reaction, or self-force, in chameleon theories on galactic scale objects. Our method used the analogy between gravitational objects with a thin shell and electrostatics, enabling us to use the methods of images to compute the back-reaction. We applied our method to the NFW profile of dark matter halos.

When we apply our results to the circular velocity of satellites in the surrounding region of the halo we have found that the back-reaction cannot be ignored. When we only included the fifth force we found that the circular velocity was the same for all objects in the exterior region surrounding the halo. This situation changes considerably upon including the back-reaction. Indeed, depending on the mass of the satellite, the back-reaction can be a large modification to the original result.

Our results suggest that there could be a violation of the equivalence principle in the outskirts of galactic haloes. While current bounds, based on the observations of the tidal streams of the Sagittarius dwarf galaxy, are not yet sensitive to this effect, future surveys of kinematics in the Milky Way halo can dramatically strengthen these limits<sup>24</sup>. This opens up another channel for testing chameleon theories. More generally our results suggest that in some of the gravitational tests for chameleon theories the back-reaction should be taken into account when putting constraints on the parameters of the theory. This is currently in progress.

### Acknowledgment

We wish to thank Justin Khoury, Louie Strigari, and Philippe Brax for discussions and useful comments. This work was supported in part by the Natural Sciences and Engineering Research Council of Canada and by STFC, UK. NA is in part supported by the Perimeter Institute for Theoretical Physics. Research at Perimeter Institute is supported by the Government of Canada through Industry Canada and by the Province of Ontario through the Ministry of Research & Innovation. ACD wishes to thank the Perimeter Institute for hospitality whilst this work was initiated.

---

<sup>1</sup> S. Perlmutter *et al.* [Supernova Cosmology Project Collaboration], *Astrophys. J.* **517**, 565 (1999) [arXiv:astro-ph/9812133].

<sup>2</sup> A. G. Riess *et al.* [Supernova Search Team Collaboration], *Astron. J.* **116**, 1009 (1998) [arXiv:astro-ph/9805201].

<sup>3</sup> E. G. Adelberger [ EOT-WASH Group Collaboration ], [hep-ex/0202008].

- <sup>4</sup> J. K. Hoskins, R. D. Newman, R. Spero, J. Schultz, Phys. Rev. **D32** (1985) 3084-3095.
- <sup>5</sup> R. S. Decca, D. Lopez, E. Fischbach, G. L. Klimchitskaya, D. E. Krause, V. M. Mostepanenko, Phys. Rev. **D75** (2007) 077101. [hep-ph/0703290].
- <sup>6</sup> B. Bertotti, L. Iess, P. Tortora, Nature **425** (2003) 374.
- <sup>7</sup> J. Khoury, A. Weltman, Phys. Rev. **D69** (2004) 044026. [astro-ph/0309411].
- <sup>8</sup> P. Brax, C. van de Bruck, A. -C. Davis, J. Khoury, A. Weltman, Phys. Rev. **D70** (2004) 123518. [astro-ph/0408415].
- <sup>9</sup> D. F. Mota and D. J. Shaw, Phys. Rev. D **75** (2007) 063501 [arXiv:hep-ph/0608078].
- <sup>10</sup> P. Brax, C. van de Bruck, A. -C. Davis, D. F. Mota, D. J. Shaw, Phys. Rev. **D76** (2007) 124034. [arXiv:0709.2075 [hep-ph]].
- <sup>11</sup> P. Brax, C. Burrage, Phys. Rev. **D83** (2011) 035020. [arXiv:1010.5108 [hep-ph]].
- <sup>12</sup> P. Brax, C. van de Bruck, A. -C. Davis, D. F. Mota, D. J. Shaw, Phys. Rev. **D76** (2007) 085010. [arXiv:0707.2801 [hep-ph]].
- <sup>13</sup> P. Brax, C. van de Bruck, A. -C. Davis, A. M. Green, Phys. Lett. **B633** (2006) 441-446. [astro-ph/0509878].
- <sup>14</sup> B. Li, H. Zhao, Phys. Rev. **D80** (2009) 044027. [arXiv:0906.3880 [astro-ph.CO]].
- <sup>15</sup> C. Burrage, A. -C. Davis, D. J. Shaw, Phys. Rev. **D79** (2009) 044028. [arXiv:0809.1763 [astro-ph]].
- <sup>16</sup> P. Brax, C. van de Bruck, A. C. Davis, D. J. Shaw, D. Iannuzzi, Phys. Rev. Lett. **104** (2010) 241101. [arXiv:1003.1605 [quant-ph]].
- <sup>17</sup> L. Hui, A. Nicolis and C. Stubbs, Phys. Rev. D **80**, 104002 (2009) [arXiv:0905.2966 [astro-ph.CO]].
- <sup>18</sup> H. Oyaizu, M. Lima and W. Hu, Phys. Rev. D **78**, 123524 (2008) [arXiv:0807.2462 [astro-ph]].
- <sup>19</sup> Y. Li and W. Hu, arXiv:1107.5120 [astro-ph.CO].
- <sup>20</sup> G. -B. Zhao, B. Li, K. Koyama, Phys. Rev. **D83** (2011) 044007. [arXiv:1011.1257 [astro-ph.CO]].
- <sup>21</sup> J. F. Navarro, C. S. Frenk and S. D. M. White, Astrophys. J. **490**, 493 (1997) [arXiv:astro-ph/9611107].
- <sup>22</sup> K. Jones-Smith and F. Ferrer, arXiv:1105.6085 [astro-ph.CO].
- <sup>23</sup> M. Kesden, M. Kamionkowski, Phys. Rev. Lett. **97**, 131303 (2006). [astro-ph/0606566].
- <sup>24</sup> M. Kesden, M. Kamionkowski, Phys. Rev. **D74**, 083007 (2006). [astro-ph/0608095].



- <sup>25</sup> M. Kesden, Phys. Rev. **D80**, 083530 (2009). [arXiv:0903.4458 [astro-ph.CO]].
- <sup>26</sup> E. L. Lokas, S. Kazantzidis, S. R. Majewski, D. R. Law, L. Mayer, P. M. Frinchaboy, Astrophys. J. **725**, 1516-1527 (2010). [arXiv:1008.3464 [astro-ph.CO]].
- <sup>27</sup> Note that this form of the potential,  $V(\phi)$ , is only assumed on large galactic scales, and thus cannot be directly compared to solar system or cosmological constraints.